Supporting Information

Synthesis of raspberry-like nanogapped Fe_3O_4@Au nanocomposites for SERS-based lateral flow detection of multiple tumor biomarkers

Wanzhu Shen[a,b], Chongwen Wang[b,c,*], Xingsheng Yang[b,c], Chaoguang Wang[e], Zihui Zhou[c], Xiaoxian Liu[b,c], Rui Xiao[b,*], Bing Gu[c,*], Shengqi Wang[a,b,*]

[b] *Anhui Medical University, Hefei 410073, PR China.*

[b] *Beijing Institute of Radiation Medicine, Beijing 100850, PR China.*

[c] *College of Life Sciences, Anhui Agricultural University, Hefei 230036, PR China.*

[d] *Department of Laboratory Medicine, Affiliated Hospital of Xuzhou Medical University, Xuzhou 221004, PR China.*

[e] *College of Mechatronics Engineering and Automation, National University of Defense Technology, Changsha 410073, P. R. China*

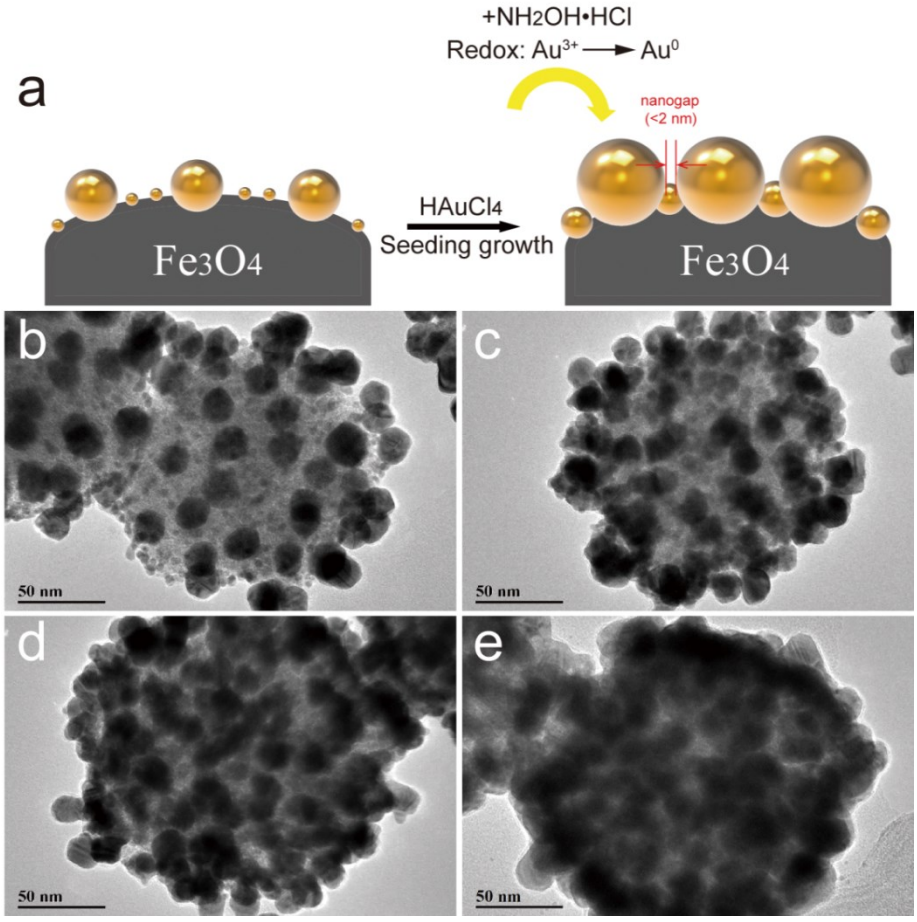

Fig. S1. (a) Schematic illustration for the fabrication of nanogapped Au shell on the Fe_3O_4 MNPs. TEM images of nanogapped RAuMNPs synthesized with different

concentration of $HAuCl_4$: (b) 0 μM, (c) 4 μM, (d) 8 μM, and (e) 16 μM, respectively.

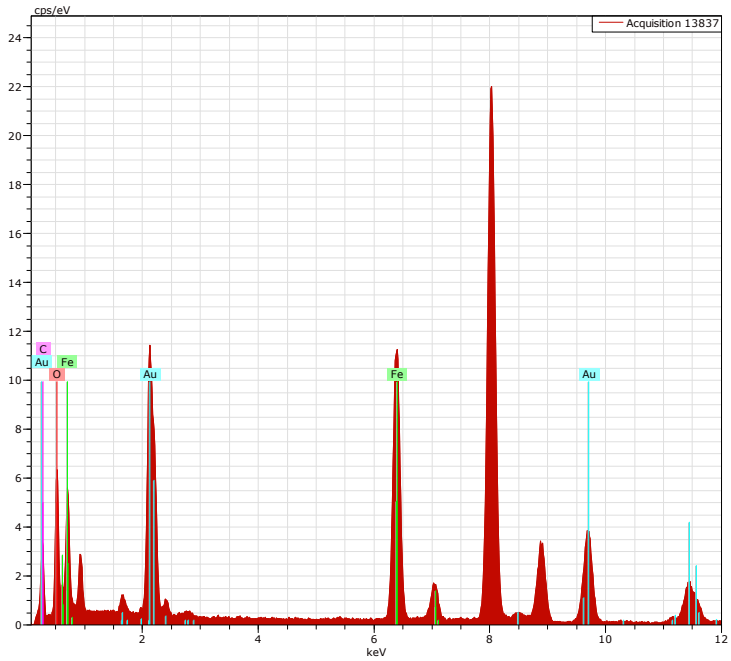

Fig. S2. EDS data from a single RAuMNP. The Cu signal is from the Cu grids of the TEM sample.

S3 EF calculation:

To quantify the enhancement ability of the RAuMNPs, the enhancement factor (EF) was calculated as the ratio of photons scattered by the SERS substrate and the normal substrate. EF was estimated according to the following equation:

$EF=(I_{SERS}/I_{bulk})(N_{bulk}/N_{SERS})$, whereas N_{bulk} and N_{SERS} is the number of molecules contributed to the Raman and SERS signal, respectively, and I_{bulk} and I_{SERS} is the respective signal intensity of the related peaks. However, intrinsic EF is difficult to estimate because several variables, such as adsorbed molecules and laser scattering volume, are difficult to obtain. In our experiment, all the other parameters, including the laser diameter, laser power, exposure time, and microscopic magnification, were identical. The chemical droplets were of the same volume, and the number of detected DTNB molecules was proportional to its concentration. Therefore, the EF was roughly estimated by comparing the intensity of the Raman peak in the SERS spectrum with that in the normal Raman spectrum according to the equation:

$EF = (I_{SERS}/I_{RS}) \times (C_{RS}/C_{SERS})$, where I_{SERS} and I_{RS} are the vibration intensities in the SERS and normal Raman spectra of DTNB molecules, and C_{RS} and C_{SERS} are the concentrations of the DTNB molecules in the reference and SERS samples,

respectively. The peak at 1332 cm^{-1} from the DTNB Raman spectrum (Fig. S3) was chosen for analysis, and the intensities for peaks from Si substrate (green line) and RAuMNPs (red line) were 3458 and 15294 a.u., respectively. The DTNB concentrations for peaks (black line and red line) were 0.5 M and 10^{-7} M, respectively. Therefore, the EF of the RAuMNPs was roughly estimated to be 2.21×10^{7}.

Moreover, the value of SERS intensity from 200 nm Fe_3O_4@Au MNPs with common Au shell (blue line) at the same DTNB concentration (10^{-7} M) was 6195 a.u., thus the EF of the common Fe_3O_4@Au MNPs was calculated to be 8.96×10^{6}. These calculations supported the fact that the EF of RAuMNPs was 2.46 times higher than that of 200 nm Fe_3O_4@Au MNPs with common Au shell.

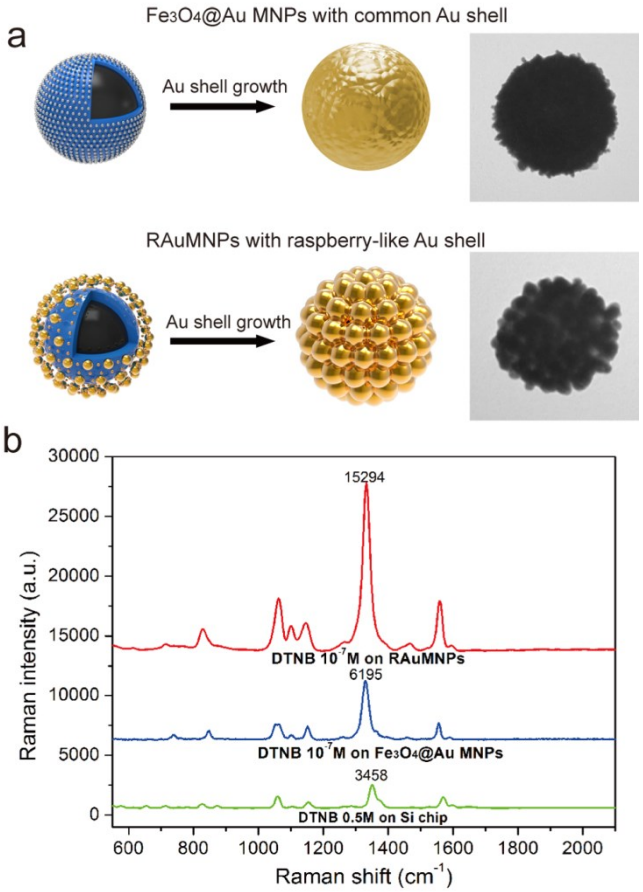

Fig. S3. (a) Different surface morphologies of RAuMNPs and Fe_3O_4@Au MNPs with common Au shell. The 200 nm Fe_3O_4@Au MNPs with common Au shell were synthesized according to our previous publication (***Wang et al, ACS Appl. Mater. Interfaces 2016, 8, 19958−19967; Wang et al, Analyst, 2016, 141, 6226–6238***). (b) Raman spectra of DTNB molecules on different substrates: 0.5 M DTNB on Si substrate (green line), 10^{-7} M DTNB on RAuMNPs (red line), and 10^{-7}M DTNB on 200 nm Fe_3O_4@Au MNPs (blue line).

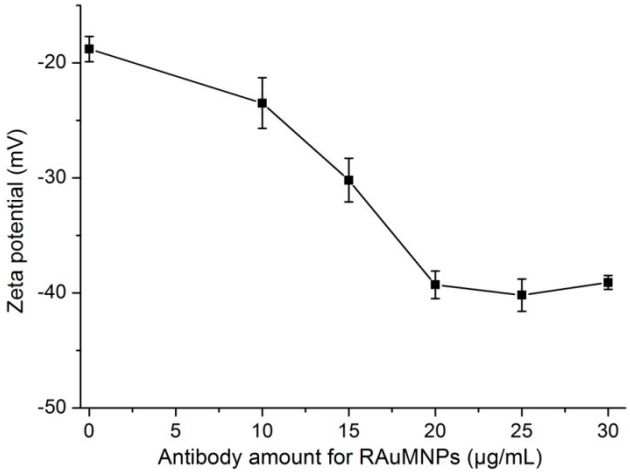

Fig. S4. Zeta potential of RAuMNPs tags versus the amount of antibody modified on their surface. The error bars represent the standard deviations from three measurements.

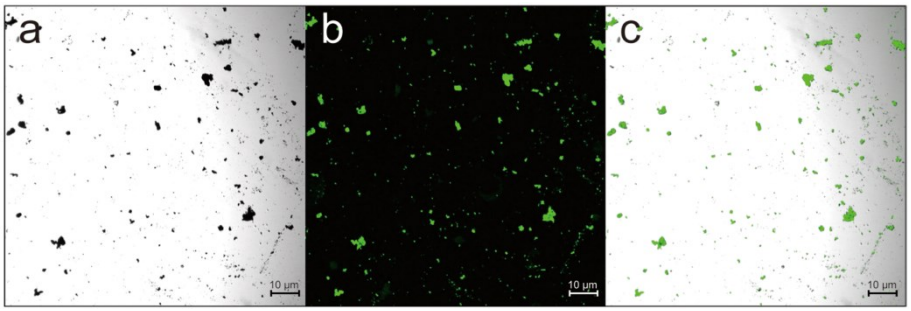

Fig. S5. (a) Brightfield, (b) fluorescence, and (c) merged images of mouse monoclonal AFP antibody-modified RAuMNPs tags conjugated with Dylight 488-labeled goat antimouse IgG.

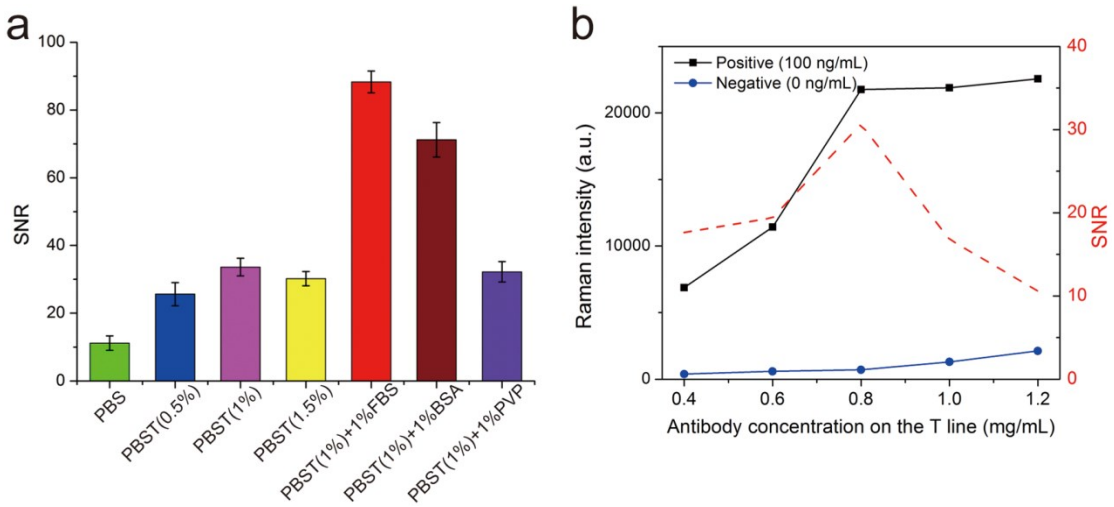

Fig. S6. (a) Optimization of running buffer on the RAuMNP tag-based SERS-LFIA. (b) Effects of detection antibody concentration on the test line.

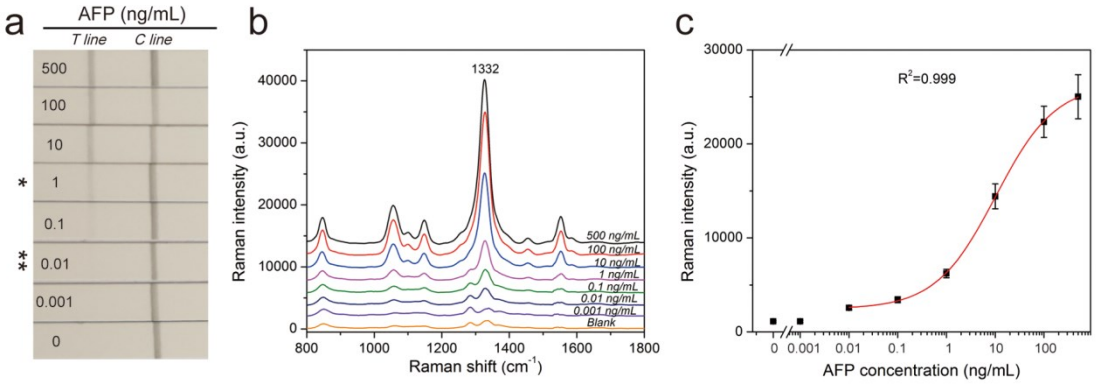

Fig. S7. (a) Photographs of the common Fe_3O_4@Au tags-based LFIA strips in the presence of different concentrations of AFP. (b) SERS spectra measured in the corresponding test lines. (c) Plot of the Raman intensity at 1332 cm^{-1} as a function of the concentration of AFP. Error bars are the standard deviation of three repetitive experiments.

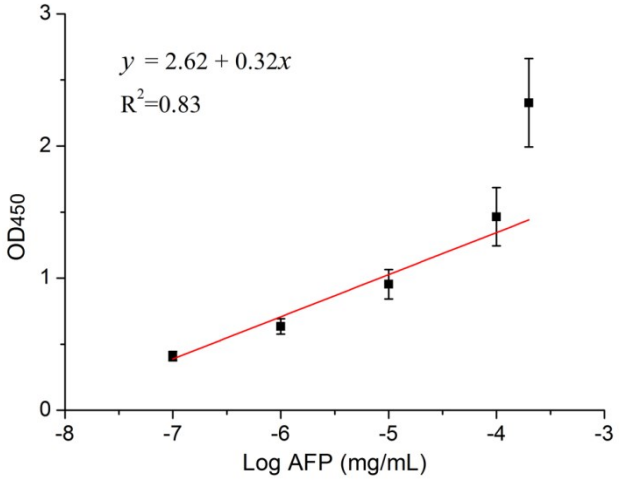

Fig. S8. ELISA analysis for different concentrations of AFP in 10% bovine serum. The error bars indicate the standard deviations calculated from three measurement.

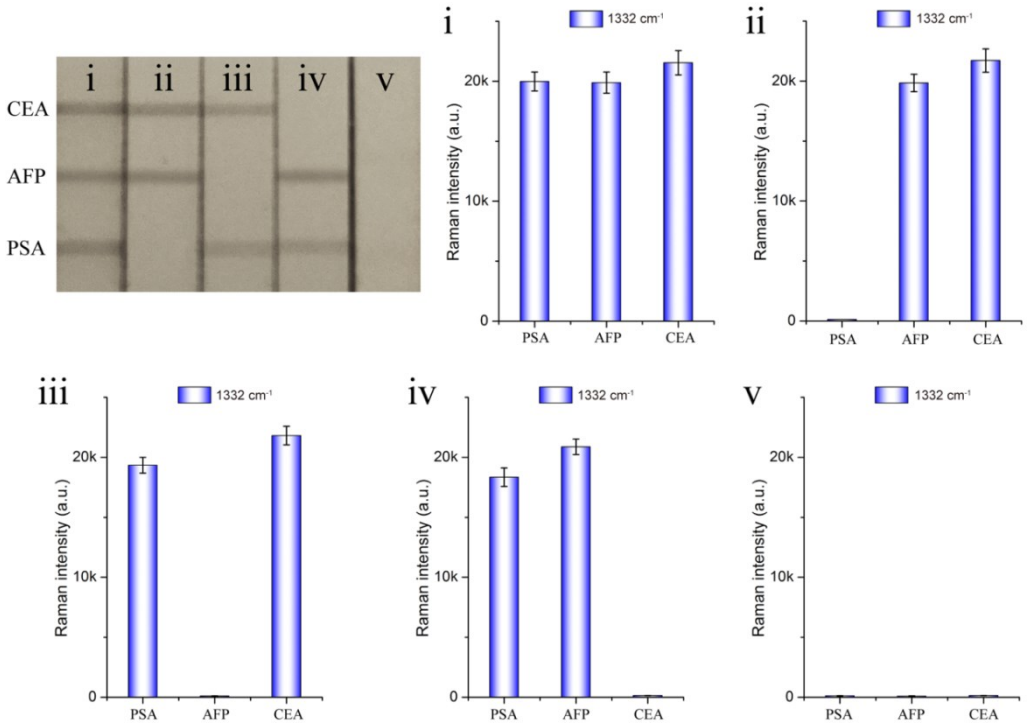

Fig. S9. Photographs and corresponding SERS intensity at 1332 cm^{-1} of the RAuMNP based SERS-LFIA in the presence of (i) PSA, 50 ng/mL; AFP, 50 ng/mL; CEA, 50 ng/mL; (ii) PSA, 0 ng/mL; AFP, 50 ng/mL; CEA, 50 ng/mL; (iii) PSA, 50 ng/mL; AFP, 0 ng/mL; CEA, 50 ng/mL; (iv) PSA, 50 ng/mL; AFP, 50 ng/mL; CEA, 0 ng/mL; (v) PSA, 0 ng/mL; AFP, 0 ng/mL; CEA, 0 ng/mL.

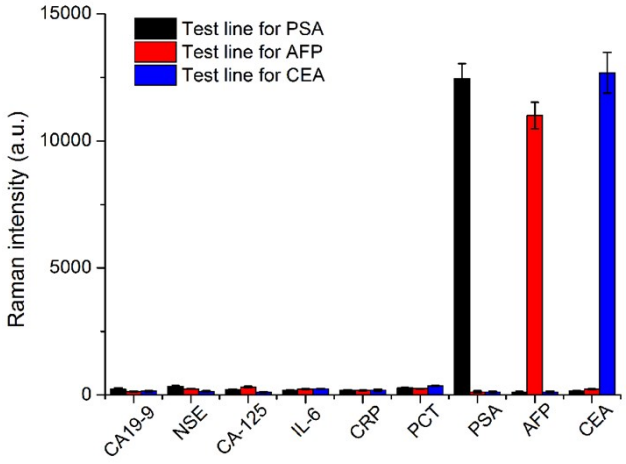

Fig. S10. Specificity of the RAuMNP based SERS-LFIA. Error bars represent the standard deviation of three repetitive experiments.

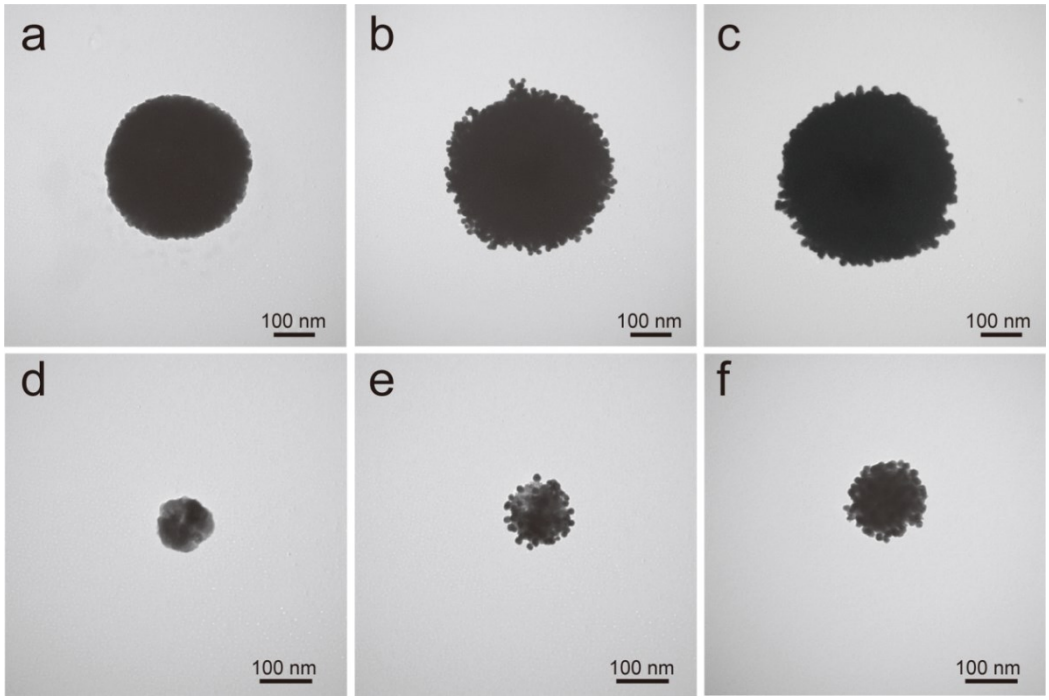

Fig. S11. TEM images of Fe_3O_4 with different sizes: (a) ~500 nm and (d) ~100 nm, and their corresponding fabricated Fe_3O_4-Au seed (20+3 nm) (b) and (e), and nanogapped Fe_3O_4@Au MNPs in (c) and (f), respectively.